PHYSICAL MODELLING OF LUMINESCENCE SPECTRA FROM CRYSTALLINE SILICON

Daniel Macdonald, AnYao Liu, Hieu T. Nguyen, Siew Yee Lim and Fiacre E. Rougieux
Research School of Engineering, The Australian National University
Canberra, ACT 2601, Australia.
email: daniel.macdonald@anu.edu.au. Phone: +61 261252973. Fax: +61 261250506.

ABSTRACT: We demonstrate that complex luminescence spectra from silicon wafers can be accurately modelled using a simple expression for the individual phonon-related components. By using combinations of various phonon emission and absorption events, it is possible to build up the entire luminescence spectra, which we demonstrate for temperatures between 78 to 300 K. At room temperature, the dominant components of the spectra are caused by emission and absorption of momentum-conserving transverse optical and transverse acoustic phonons. Secondary phonon replicas also involve the emission of non-momentum-conserving inter-valley phonons. The model correctly reproduces the changes in sharpness of the measured spectra as a function of temperature, as well as correctly accounting for the relative change in impact of phonon emission and absorption related luminescence. At low temperatures, additional peaks caused by recombination through neutral dopant atoms are also evident, and can be modelled using the same approach. The model may be useful for understanding luminescence spectra from silicon wafers and solar cells.
Keywords: silicon, photoluminescence, modelling

1 INTRODUCTION

Spectrally-resolved luminescence measurements are proving to be of increasing interest for silicon solar cell research and development. Some established and recent applications include: accurate determination of fundamental properties such as band-gap narrowing [1], absorption and radiative recombination coefficients [2-4]; determination of carrier diffusion lengths, carrier profiles and lifetimes [5-7]; characterising surface texture and light-trapping properties [8,9]; studying the properties of dislocations via D-line emission [10]; and identification of locally doped regions [11,12].

These applications stem from the fact that the shape of the band-to-band luminescence peak contains rich information about the optical properties, doping concentrations, and carrier profiles within a wafer or device. To access this information, the spectra are often modelled via knowledge of the absorption coefficient. However, this approach does not provide insight into the underlying carrier-phonon-photon interactions which give rise to the detailed structure of the band-to-band peak. In this paper we present a simple physical model which allows the shape of the band-to-band peak to be reconstructed using a combination of simple components, each representing a particular phonon interaction, and which clearly reveals the underlying physical processes. Despite its simplicity, the model is found to be applicable across a wide range of temperatures, from 78K up to room temperature. In addition to being of intrinsic interest, is likely to be useful in future applications of spectral luminescence for silicon solar cells.

2 BACKGROUND

For an indirect semiconductor such as silicon, band-to-band optical absorption or emission must be accompanied by the simultaneous absorption or emission of one or more phonons, in order to conserve momentum. The energy of the absorbed or emitted photon then depends on the band-gap energy and the energy of the phonon(s) involved. Firstly considering optical absorption, for semiconductors with parabolic densities of states near the band edges, the optical absorption coefficient α, accompanied by the simultaneous absorption or emission of a single phonon of energy E_{phonon}, can then be approximated by [13,14]:

$$\alpha = A \left[\frac{(h\nu - E_{gap} - E_{phonon})^2}{1 - \exp(-E_{phonon}/kT)} + \frac{(h\nu - E_{gap} + E_{phonon})^2}{\exp(-E_{phonon}/kT) - 1} \right]$$

where $h\nu$ is the photon energy, E_{gap} the minimum band-gap energy and A is a constant. Note that the first term corresponds to optical absorption via phonon emission, and the second term to optical absorption via phonon absorption. Macfarlane et $al.$ used these expressions to accurately model their measurements of the absorption coefficients of both Si and Ge near the band-gap energy [14-16].

In this work we use the terms in the expression above to model the optical $emission$ from silicon. Analogous expressions for emission can be obtained by multiplying the terms in the equation above by the factor $\exp(-h\nu/kT)$. Furthermore, we also extend the model to account for multiple phonon processes, namely optical emission via the simultaneous absorption/emission of two or more phonons.

3 EXPERIMENTAL DETAILS

The sample investigated in the work was a 220 micron thick, $3\Omega.cm$ phosphorus doped n-type float-zone wafer, passivated by PECVD SiN films, with minority carrier diffusion lengths much longer than the sample thickness, leading to spatially uniform excess carrier profiles (see Ref. [3] for more details). The sample was excited with a 785nm laser diode with on-sample power of 250 mW and a beam diameter of 2.2mm. The resulting photoluminescence was detected with a liquid-nitrogen cooled InGaAs detector via a double-grating monochromator. The laser beam was mechanically chopped at 500Hz, and the signal from the detector was recovered using a lock-in amplifier for improved sensitivity. The sample temperature was controlled precisely with a liquid-nitrogen cooled cryostat, allowing measurements in the range from 78 to 300 K. The spectra

were measured with 5 nm spectral resolution, and a typical integration time of 10 seconds per data point. More details can be found in Ref. [3].

4   RESULTS AND DISCUSSION

Figure 1 shows the normalised PL spectra measured at temperatures of 78, 170 and 300 K. The spectra have been corrected for photon re-absorption using absorption coefficient data from Ref [3]. We found that re-absorption does have some impact on the data at 300 K for photon energies greater than the peak value, although its impact at the lower temperatures is negligible. Note that the spectra become sharper with more distinct peaks and shoulders as the temperature is reduced.
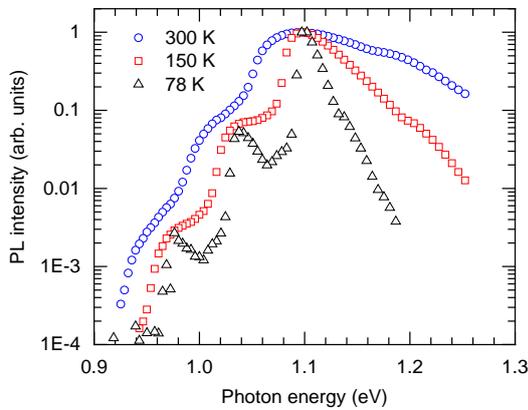

Figure 1: Normalised PL spectra from a passivated n-type silicon wafer at various temperatures. Note that the spectra are corrected for photon re-absorption.

Figure 2 shows our fitting of the 300 K spectra using the equation presented above. We find that a total of eight components are required to obtain a good overall fit, which comprise combinations of four different phonons. The four phonon types and their energies are shown in Table I. When modelling the effect of multiple phonon emission, the sum of the phonon energies is used in the equation.
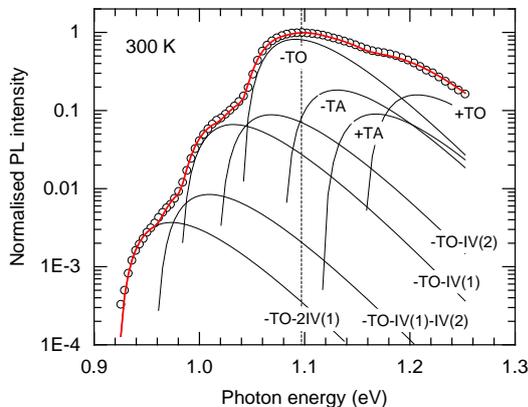

Figure 2: Normalised PL spectra at 300 K with eight modelled components. The total fit is shown as a red line. The modelled band-gap is shown as a vertical dashed line. The energies of the various phonons are listed in Table I.

Table I: Phonon types and energies used in the fitting procedure. The TO and TA phonon energies are taken from Ref [17].

Phonon	Energy (meV)	Momentum conserving?
Transverse optical - TO	58.0	yes
Transverse acoustic - TA	18.4	yes
Inter-valley type 1 - IV(1)	60	no
Inter-valley type 2 - IV(2)	23	no

Due to the indirect band-gap of silicon, each fit component must include one momentum-conserving phonon. In this work we have used either a transverse optical (TO) or a transverse acoustic (TA) phonon. These phonons may either be emitted (indicated by – TO, for example), or absorbed (+ TO), leading to four of the eight components used in the total fit, as shown in Figure 1. The energies used for the TO and TA phonons are taken from Vouk and Lightowlers [17]. Note that the low energy edge of each component is separated from the band-gap energy by an amount equal to the relevant phonon energy, with emission processes located on the low energy side of the band-gap, and absorption processes on the high energy side.

The other four components used in the fits are replicas of the – TO peak. These components involve the emission of a TO phonon, plus the emission of one or more non-momentum conserving phonon(s). Here we have used two types of non-momentum conserving phonons labeled as IV(1) and IV(2). There are many non-momentum conserving inter-valley (IV) phonons reported in the literature (see References [17,18] for example), some of which have energies similar to those required in our fitting, as well as obeying the required selection rules. However, they have mostly been studied at lower temperatures than used here, hence it is not trivial to assign our IV(1) and IV(2) phonons to those identified previously. The identification of these phonons is a topic of ongoing enquiry. Initial efforts indicate that the often cited Raman phonon has an energy slightly too high (64.4 meV) to give good fits to our spectra.

We note that other combinations of the four phonon types listed in Table I can also occur - for example -TA-IV(1). Evidently, however, they have little impact on the total spectrum.

With the phonon energies from Table I, the only other fit parameters used in the modelling are a scaling factor for each component, and the band-gap energy, as we find that literature values for the band-gap do not give a reasonable global fit. Indeed the modelling approach used here can in principle provide a very accurate way of determining band-gap energies for indirect semiconductors, as has been applied before for heavily-doped silicon, for example in [1]. Our values for the band-gap energies derived from the fit procedure shown here will be reported elsewhere. The scaling factors may also yield interesting information about the relative phonon densities as a function of temperature.

Figures 3 and 4 show the corresponding fits for the 170 K and 78 K spectra respectively. For the 170K case,

we have used the same eight components as for 300 K, while for 78 K we did not require the +TO peak, and so only seven components were used. For both temperatures we find a very good fit using only minor adjustments to the scaling factors, although for 78 K there are some visible discrepancies in between the phonon replicas, at around 1.0 and 1,08 eV. This is discussed further below. Note that the fitted values of the band-gap energies have shifted noticeably, as indicated in the plots.

It is interesting to note that the simple expression used in this work accurately accounts for the sharpening of the PL spectra as the temperature is decreased. Further, the term in the denominator represents the change in phonon densities as the temperature changes, and this term correctly accounts for the very strongly reduced impact of the phonon absorption related components, occurring on the high energy side of the spectra, as the temperature decreases. This reflects the fact that fewer phonons are present to be absorbed at lower temperatures, and so phonon emission events become more dominant, relatively speaking.
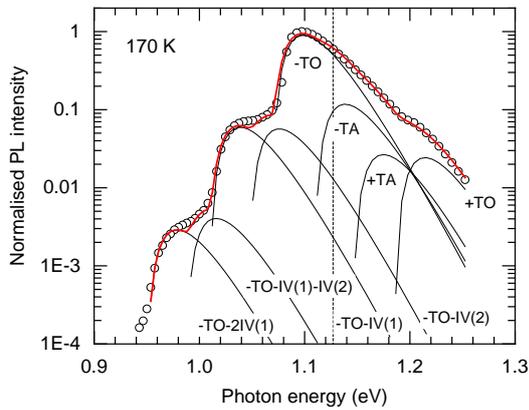

Figure 3: Normalised PL spectra at 170 K with the same eight modelled components as Figure 2. The total fit is shown as a red line. The modelled band-gap is shown as a vertical dashed line.
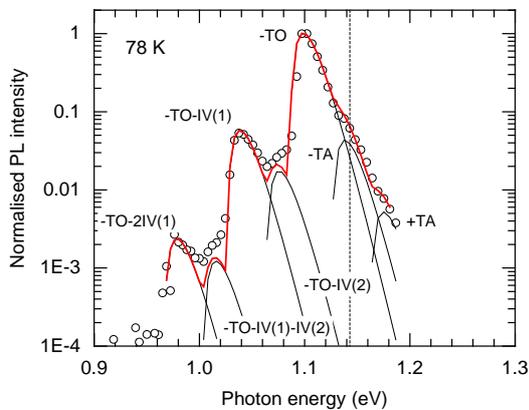

Figure 4: Normalised PL spectra at 78 K with seven modelled components (no +TO component). The total fit is shown as a red line. The modelled band-gap is shown as a vertical dashed line. Note the incorrect fit at around 1.0 and 1.08 eV.

The slightly incorrect fitting in Figure 4 between the phonon replicas, at around 1.0 and 1,08 eV, is caused by additional transitions related to recombination through neutral dopant atoms [4,18]. Peaks at the same energies have been reported previously at 80 K by Dean *et al*. [18], who attributed them to recombination through neutral phosphorus atoms. Naturally these events become very much diminished as the temperature is increased, due to thermal ionization of the dopants. Figure 5 shows that we can include the effect of these additional peaks, shown as four dashed red lines, to once again obtain a very good overall fit. In increasing energy, they are attributed to $P_3 - TO - IV(1)$, $P_1 - TO - IV(1)$, $P_3 - TO$, and $P_1 - TO$, where the use of P_1 and P_3 follows the notation used by Dean *et al*. Naturally the relative intensity of these peaks should increase as the dopant concentration increases, which we have indeed observed in our initial measurements.
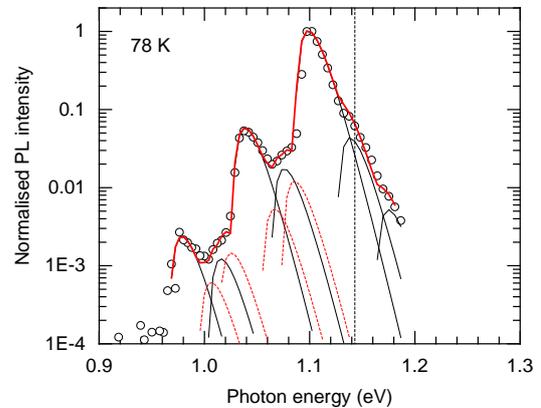

Figure 5: Normalised PL spectra at 78 K with the seven modelled components from Figure 4, plus an additional four dopant-related components shown as dashed red lines. The total fit is shown as a solid red line. The modelled band-gap is shown as a vertical dashed line.

5 CONCLUSIONS

A simple physical model for the luminescence emission from silicon is shown to provide a good fit to PL spectra measured at temperatures between 78 and 300 K. The model allows the contributions of specific combinations of phonons to be easily accounted for and combined. It accurately reproduces the changes in sharpness of the spectra as a function of temperature, and also accounts for the changing impact of phonon absorption events relative to emission events. At low temperatures around 78 K, it is necessary to also include emission events related to recombination via neutral dopant atoms. A more complete account of this work is currently in preparation, including a more definite identification of the inter-valley phonons, and a description of the extracted band-gap energies.

6 ACKNOWLEDGMENTS

7   REFERENCES

[1] J. Wagner, Phys. Rev. B, 32, (1985) 1323.
[2] T. Trupke, M. A. Green, P. Wurfel, P. P. Altermatt, A. Wang, J. Zhao and R. Corkish, Temperature dependence of the radiative recombination coefficient of intrinsic crystalline silicon, J. Appl. Phys. , 94, (2003) 4930.
[3] H. T. Nguyen, F. E. Rougieux, B. Mitchell and D. Macdonald, Temperature dependence of the band-band absorption coefficient in crystalline silicon from photoluminescence, J. Appl. Phys., 115, (2014) 043710.
[4] E. Daub and P. Wurfel, Ultralow values of the absorption coefficient of Si obtained from luminescence, Phys. Rev. Lett. , 74, (1995) 1020.
[5] P. Wurfel, T. Trupke, T. Puzzer, E. Schaffer, W. Warta and S. W. Glunz, Diffusion lengths of silicon solar cells from luminescence images, J. Appl. Phys., 101, (2007) 123110.
[6] H. T. Nguyen, F. E. Rougieux, S. C. Baker-Finch and D. Macdonald, Impact of Carrier Profile and Rear-Side Reflection on Photoluminescence Spectra in Planar Crystalline Silicon Wafers at Different Temperatures, IEEE J. Photovoltaics, 5, (2015) 77.
[7] B. Mitchell, M. K. Juhl, M.A.Green and T. Trupke, Full spectrum photoluminescence lifetime analyses on silicon bricks, IEEE J. Photovoltaics, 3, (2013) 962.
[8] C. Schinke, D. Hinken, J. Schmidt, K. Bothe and R. Brendel, IEEE J. Photovoltaics, 3, (2013) 1038.
[9] C. Barugkin, Y. Wan, D. Macdonald and K. R. Catchpole, Evaluating plasmonic light trapping with photoluminescence, IEEE J. Photovoltaics, 3, (2013) 1292.
[10] M. Tajima, Spectroscopy and topography of deep-level luminescence in photovoltaic silicon, IEEE Journal of Photovoltaics, 4, (2014) 1452.
[11] H. T. Nguyen, D. Yan, F. Wang, P. Zheng, Y. Han and D. Macdonald, Micro-photoluminescence spectroscopy on heavily doped layers of silicon solar cells, Physica Status Solidi – Rapid Research Letters, 9 (4), (2015) 230.
[12] P. Gundel, D. Suwito, U. Jäger, F. D. Heinz, W. Warta and M. C. Schubert, IEEE Trans. Elec. Devices, 58, (2011) 2874.
[13] R. A. Smith, Semiconductors, (Cambridge Press, 1959).
[14] G. G. Macfarlane and V. Roberts, Infrared Absorption of Germanium near the Lattice Edge, Physical Review, 97, (1955) 1714.
[15] G. G. Macfarlane and V. Roberts, Infrared Absorption of Silicon Near the Lattice Edge, Physical Review, (1955) 1865.
[16] G. G. Macfarlane, T. P. Mclean, J. E. Quarrington and V. Roberts, Fine Structure in the Absorption-Edge Spectrum of Si, Physical Review, 111, (1958) 1245.
[17] M. A. Vouk and E. C. Lightowlers, Two-phonon assisted free exciton recombination radiation from intrinsic silicon, Journal of Physics C: Solid State Physics, 10, (1977) 3689.
[18] P. J. Dean, J. R. Haynes and W. F. Flood, New radiative recombination processes involving neutral donors and acceptors in silicon and germanium, Physical Review, 161, (1967) 711.